Stationary and dynamical properties of finite N-unit Langevin models subjected to multiplicative noises

Hideo Hasegawa ¹

Department of Physics, Tokyo Gakugei University Koganei, Tokyo 184-8501, Japan

(March 23, 2022)

Abstract

We have studied the finite N-unit Langevin model subjected to multiplicative noises, by using the augmented moment method (AMM), as a continuation of our previous paper [H. Hasegawa, J. Phys. Soc. Jpn. **75** (2006) 033001]. Effects of couplings on stationary and dynamical properties of the model have been investigated. The difference and similarity between the results of diffusive and sigmoid couplings are studied in details. Time dependences of average and fluctuations in local and global variables calculated by the AMM are in good agreement with those of direct simulations (DSs). We also discuss stationary distributions of local and global variables with the use of the Fokker-Planck equation (FPE) method and DSs. It is demonstrated that stationary distributions show much variety when multiplicative noise and external inputs are taken into account.

PACS No. 05.10.Gg, 05.45.-a, 84.35.+i

¹E-mail address: hasegawa@u-gakugei.ac.jp

1 INTRODUCTION

The Langevin equation has been widely employed as a useful model for a wide range of stochastic phenomena. Much study has been made on the Langevin model for a single unit as well as coupled systems (for a recent review, see Ref. [1]). The Langevin equation has been commonly solved by using the Fokker-Planck equation (FPE) method [2]. For N-unit Langevin equations, the FPE method leads to (N+1)-dimensional partial equations to be solved with proper boundary conditions, which is usually very difficult. Direct simulation (DS) requires the computational time which grows as N^2 with increasing N. As a useful semi-analytical method for stochastic equations, Rodriguez and Tuckwell [3] proposed the moment method in which the first and second moments of variables are taken into account. In this approach, original N-dimensional Langevin equations are transformed to (N/2)(N+3)-dimensional deterministic equations. For example, this figure becomes 65 and 5150 for N=10 and N=100, respectively. Based on a macroscopic point of view, Hasegawa [4] has proposed the augmented moment method (AMM), in which the dynamics of coupled Langevin equations is described by a fairly small number (three) of quantities: averages and fluctuations of local and global variables. The AMM has been successfully applied to a study on the dynamics of coupled stochastic systems described by Langevin, FitzHugh-Nagumo and Hodgkin-Huxley models subjected to additive noises with global, local or small-world couplings (with and without transmission delays) [5]-[9]. The AMM was originally developed by expanding variables around their mean values in the stochastic model in order to obtain the second-order moments both for local and global variables [4]. In a recent paper [10], we have reformulated the AMM with the use of the FPE, in order to apply the AMM to coupled Langevin model subjected to multiplicative noises, in which the difficulty of the Ito versus Stratonovich representations is inherent.

In recent years, much attention has been paid to multiplicative noises in addition to additive noises (for a review of study on multiplicative noises, see Ref. [11], related references therein). The stationary distribution of the Langevin model subjected to multiplicative noises has been considerably investigated in various contexts [11]-[15]. Interesting phenomena caused by the two noises have been intensively studied. It has been realized that the property of multiplicative noises is different from that of additive noises in some respects. (1) Multiplicative noises induce the phase transition, creating an ordered state, while additive noises are against the ordering [16]-[20]. (2) Although the probability distribution in stochastic systems subjected to additive Gaussian noise follows the

Gaussian, multiplicative Gaussian noises generally yield non-Gaussian distribution [12]-[15][21, 22]. (3) The scaling relation of the effective strength for additive noise given by $\beta(N) = \beta(1)/\sqrt{N}$ is not applicable to that for multiplicative noise: $\alpha(N) \neq \alpha(1)/\sqrt{N}$, where $\alpha(N)$ and $\beta(N)$ denote effective strengths of multiplicative and additive noises, respectively, in the N-unit system [10]. A naive approximation of the scaling relation for multiplicative noise: $\alpha(N) = \alpha(1)/\sqrt{N}$ as adopted in Ref. [20] yields the result which does not agree with that of DSs.

The purpose of the present paper is to discuss effects of couplings on stationary and dynamical properties of the N-unit Langevin model with multiplicative noises, which has been not investigated in [10]. The paper is organized as follows. In Section 2, the AMM is employed for a discussion on the finite-N Langevin model which is subjected to additive and multiplicative noises and which is coupled by diffusive and sigmoid couplings. Numerical results are presented in Section 3. Section 4 is devoted to discussion and conclusion, where the stationary distribution of local and global variables are studied with the FPE and DS.

2 AUGMENTED MOMENT METHOD

2.1 A Generalized Langevin model

We have adopted the finite N-unit Langevin model given by

$$\frac{dx_i}{dt} = F(x_i) + \alpha G(x_i)\eta_i(t) + \beta \xi_i(t) + I_i^{(c)}(t) + I^{(e)}(t), \tag{1}$$

with

$$I_i^{(c)}(t) = \frac{J}{Z} \sum_{k(\neq i)} [x_k(t) - x_i(t)] + \frac{K}{Z} \sum_{k(\neq i)} H(x_k(t)), \qquad (i = 1 - N)$$
 (2)

and

$$H(x) = \frac{x}{\sqrt{x^2 + 1}}. (3)$$

Here F(x) and G(x) denote arbitrary functions of x: J and K express the diffusive and sigmoid couplings, respectively, whose effects will be separately discussed in Sections 2.2 and 2.3: Z (= N - 1) stands for the coordination number: $I^{(e)}(t)$ is an external input: α and β denote the strengths of multiplicative and additive noises, respectively, and $\eta_i(t)$ and $\xi_i(t)$ express zero-mean Gaussian white noises with correlations given by

$$\langle \eta_i(t) \, \eta_j(t') \rangle = \delta_{ij} \delta(t - t'),$$
 (4)

$$\langle \xi_i(t) \, \xi_j(t') \rangle = \delta_{ij} \delta(t - t'), \tag{5}$$

$$\langle \eta_i(t) \, \xi_i(t') \rangle = 0. \tag{6}$$

Although various types of sigmoid functions such as $\tanh(x)$ and $1/[1 + \exp(x)]$, etc. have been employed in the literature, we here adopt a simple analytical expression given by Eq. (3) [23].

The Fokker-Planck equation for the distribution of $\hat{p}(\{x_i\},t)$ is given by [24]

$$\frac{\partial}{\partial t} \hat{p}(\{x_i\}, t) = -\sum_{k} \frac{\partial}{\partial x_k} \{ [F(x_k) + \frac{\phi \alpha^2}{2} G'(x_k) G(x_k) + I_k] \hat{p}(\{x_i\}, t) \}
+ \frac{1}{2} \sum_{k} \frac{\partial^2}{\partial x_k^2} \{ [\alpha^2 G(x_k)^2 + \beta^2] \hat{p}(\{x_i\}, t) \},$$
(7)

where $I_k = I_k^{(c)} + I^{(e)}$, G'(x) = dG(x)/dx, and $\phi = 1$ and 0 in the Stratonovich and Ito representations, respectively. The averaged, global variable X(t) is given by

$$X(t) = \frac{1}{N} \sum_{i} x_i(t), \tag{8}$$

for which the Fokker-Planck equation P(X,t) is formally given by

$$P(X,t) = \int \cdots \int \prod_{i} dx_{i} \, \hat{p}(\lbrace x_{i} \rbrace, t) \, \delta\left(X - \frac{1}{N} \sum_{i} x_{i}\right). \tag{9}$$

We will discuss the property of the coupled Langevin model with the use of the AMM, which is the second-moment theory for local and global variables [4, 10]. The moments of local and global variables are defined by

$$\langle x_i^k \rangle = \int \Pi_i \, dx_i \, \hat{p}(\{x_i\}, t) \, x_i^k, \tag{10}$$

$$\langle X^k \rangle = \int dX P(X,t) X^k. \qquad (k=1,2,\cdots)$$
 (11)

From Eqs. (1), (7), (8), (10) and (11), equations of motions for mean, variance and covariance of local variable (x_i) and global variable (X) are given by [10]

$$\frac{d\langle x_i \rangle}{dt} = \langle F(x_i) \rangle + \langle I_i \rangle + \frac{\phi \alpha^2}{2} \langle G'(x_i) G(x_i) \rangle, \tag{12}$$

$$\frac{d\langle x_i \, x_j \rangle}{dt} = \langle x_i \, F(x_j) \rangle + \langle x_j \, F(x_i) \rangle + \langle x_i I_j \rangle + \langle x_j I_i \rangle$$

$$+ \frac{\phi \alpha^2}{2} [\langle x_i G'(x_j) G(x_j) \rangle + \langle x_j G'(x_i) G(x_i) \rangle]$$

$$+ [\alpha^2 \langle G(x_i)^2 \rangle + \beta^2] \delta_{ij}, \qquad (13)$$

$$\frac{d\langle X\rangle}{dt} = \frac{1}{N} \sum_{i} \frac{d\langle x_i \rangle}{dt},\tag{14}$$

$$\frac{d\langle X^2 \rangle}{dt} = \frac{1}{N^2} \sum_{i} \sum_{j} \frac{d\langle x_i \, x_j \rangle}{dt},\tag{15}$$

where $I_i = I_i^{(c)} + I^{(e)}$. Equation (12) is adopted in the mean-field approximation [17]. In Ref. [19], Eqs. (12) and (13) are employed for a discussion on the fluctuation-induced phase transition in infinite-N stochastic systems. Equations (14) and (15) play a crucial role in discussing finite-N systems, as will be shown shortly.

In the AMM [4, 10], we take into account the three quantities: μ , γ and ρ expressing the mean of X, the averaged fluctuations in local variables (x_i) and fluctuations in global variable (X), respectively, which are defined by

$$\mu = \langle X \rangle = \frac{1}{N} \sum_{i} \langle x_i \rangle, \tag{16}$$

$$\gamma = \frac{1}{N} \sum_{i} \langle (x_i - \mu)^2 \rangle, \tag{17}$$

$$\rho = \langle (X - \mu)^2 \rangle. \tag{18}$$

Expanding x_i in Eqs. (12)-(15) around the average value of μ as

$$x_i = \mu + \delta x_i, \tag{19}$$

(21)

and retaining up to the order of $\langle \delta x_i \delta x_j \rangle$, we get equations of motions for μ , γ and ρ given by

$$\frac{d\mu}{dt} = f_0 + f_2\gamma + K[h_0 + h_2\gamma] + \left(\frac{\phi \alpha^2}{2}\right) [g_0g_1 + 3(g_1g_2 + g_0g_3)\gamma] + I^{(e)}, \quad (20)$$

$$\frac{d\gamma}{dt} = 2f_1\gamma + \left(\frac{2JN}{Z}\right)(\rho - \gamma) + \left(\frac{2Kh_1N}{Z}\right)\left(\rho - \frac{\gamma}{N}\right) + (\phi + 1)(g_1^2 + 2g_0g_2)\alpha^2\gamma + \alpha^2g_0^2 + \beta^2,$$

$$\frac{d\rho}{dt} = 2f_1\rho + 2Kh_1\rho + (\phi + 1)(g_1^2 + 2g_0g_2)\alpha^2\rho + \frac{\alpha^2g_0^2}{N} + \frac{\beta^2}{N},$$
(22)

where $f_{\ell} = (1/\ell!)\partial^{\ell}F(\mu)/\partial x^{\ell}$, $g_{\ell} = (1/\ell!)\partial^{\ell}G(\mu)/\partial x^{\ell}$, and $h_{\ell} = (1/\ell!)\partial^{\ell}H(\mu)/\partial x^{\ell}$. Original N-dimensional stochastic equations given by Eqs. (1)-(3) are transformed to three-dimensional deterministic equations given by Eqs. (20)-(22). The stability of Eqs. (20)-(22) may be examined by calculating their Jacobian matrix, as will be discussed shortly. We note that equations of motions for μ and ρ in Eqs. (20) and (22) do not include the term of J for diffusive coupling, while they include the term of K for the sigmoid coupling. This is because the average of $\sum_{i}\langle I_{i}\rangle$ and $\sum_{ij}\langle x_{i}I_{j}\rangle$ in Eqs. (12) and (15) vanish due to the nature of the diffusive coupling given in Eq. (2). If we consider the conditional average of $\langle x_{i}\rangle_{i}$ for a given site i, its equation of motion has a term relevant to the coupling J, as discussed in Ref. [18].

2.2 Diffusive couplings

For the linear Langevin model given by $F(x) = -\lambda x$ and G(x) = x with diffusive couplings $(J \neq 0, K = 0)$, we get equations of motions for μ , γ and ρ in the Stratonovich representation $(\phi = 1)$ given by

$$\frac{d\mu}{dt} = -\lambda\mu + \frac{\alpha^2\mu}{2} + I^{(e)},\tag{23}$$

$$\frac{d\gamma}{dt} = -2\lambda\gamma + \left(\frac{2JN}{Z}\right)(\rho - \gamma) + 2\alpha^2\gamma + \alpha^2\mu^2 + \beta^2, \tag{24}$$

$$\frac{d\rho}{dt} = -2\lambda\rho + 2\alpha^2\rho + \frac{\alpha^2\mu^2}{N} + \frac{\beta^2}{N}.$$
 (25)

The stability of the stationary solutions given by Eqs. (23)-(25) may be examined by calculating their Jacobian matrix. We get three eigenvalues of $\lambda - \alpha^2/2$, $2\lambda - 2\alpha^2 + 2JN/Z$ and $2\lambda - 2\alpha^2$, from which the stability condition of the stationary solution is given by $\alpha^2 < \lambda$. The stable stationary solutions for $I^{(e)} = I$ are given by

$$\mu = \frac{I}{(\lambda - \alpha^2/2)},\tag{26}$$

$$\gamma = \frac{(\alpha^2 \mu^2 + \beta^2)[1 + J/Z(\lambda - \alpha^2)]}{2(\lambda - \alpha^2 + JN/Z)},$$
(27)

$$\rightarrow \frac{(\alpha^2 \mu^2 + \beta^2)}{2(\lambda - \alpha^2 + J)}, \quad (as N \to \infty)$$
 (28)

$$\rho = \frac{(\alpha^2 \mu^2 + \beta^2)}{2N(\lambda - \alpha^2)},\tag{29}$$

$$\frac{\rho}{\gamma} = \frac{1}{N} \left(\frac{\lambda - \alpha^2 + JN/Z}{\lambda - \alpha^2 + J/Z} \right), \tag{30}$$

$$\rightarrow \frac{1}{N} \left(\frac{\lambda - \alpha^2 + J}{\lambda - \alpha^2} \right). \quad (as N \to \infty)$$
 (31)

2.3 Sigmoid couplings

We will make an analysis of the linear Langevin model with $F(x) = -\lambda x$ and G(x) = x for sigmoid couplings $(J = 0, K \neq 0)$ in Eqs. (2) and (3), for which equations of motion for μ , γ and ρ in the Stratonovich representation are given by

$$\frac{d\mu}{dt} = -\lambda \mu + \frac{\alpha^2 \mu}{2} + K(h_0 + h_2 \gamma) + I^{(e)}, \tag{32}$$

$$\frac{d\gamma}{dt} = -2\lambda\gamma + \left(\frac{2Kh_1N}{Z}\right)\left(\rho - \frac{\gamma}{N}\right) + 2\alpha^2\gamma + \alpha^2\mu^2 + \beta^2,\tag{33}$$

$$\frac{d\rho}{dt} = -2\lambda\rho + 2\alpha^2\rho + 2Kh_1\rho + \frac{\alpha^2\mu^2}{N} + \frac{\beta^2}{N},\tag{34}$$

where $h_0 = \mu/\sqrt{\mu^2 + 1}$, $h_1 = 1/(\mu^2 + 1)^{3/2}$ and $h_2 = -(3\mu/2)/(\mu^2 + 1)^{5/2}$. The stationary solutions with $I^{(e)} = I$ for a small μ for which $H(\mu) \sim \mu$ are given by

$$\mu = \frac{I}{(\lambda - \alpha^2/2 - K)},\tag{35}$$

$$\gamma = \frac{(\alpha^2 \mu^2 + \beta^2)[1 + K/Z(\lambda - \alpha^2 - K)]}{2(\lambda - \alpha^2 + K/Z)},$$
(36)

$$\rightarrow \frac{(\alpha^2 \mu^2 + \beta^2)}{2(\lambda - \alpha^2)}, \quad (as N \to \infty)$$
 (37)

$$\rho = \frac{(\alpha^2 \mu^2 + \beta^2)}{2N(\lambda - \alpha^2 - K)},\tag{38}$$

$$\frac{\rho}{\gamma} = \frac{1}{N} \left(\frac{\lambda - \alpha^2 + K/Z}{\lambda - \alpha^2 - K + K/Z} \right), \tag{39}$$

$$\rightarrow \frac{1}{N} \left(\frac{\lambda - \alpha^2}{\lambda - \alpha^2 - K} \right). \quad (as N \to \infty)$$
 (40)

Three eigenvalues of Jacobian matrix relevant to Eqs. (35), (36) and (38) are $\lambda - \alpha^2/2 - K$, $\lambda - \alpha^2 - K$ and $\lambda - \alpha^2 + K/Z$, from which we get the stability condition of $\alpha^2 < \lambda - K$.

2.4 Comparison between diffusive and sigmoid couplings

Comparing Eqs. (23)-(25) for the diffusive coupling with Eqs. (32)-(34) for the sigmoid coupling, we note the following difference and similarity in μ , γ and ρ .

- (i) μ for the diffusive coupling is independent of the coupling (J) while μ for the sigmoid coupling depends on its coupling (K).
- (ii) When the (positive) coupling is introduced, γ for the diffusive coupling is decreased while γ for the sigmoid coupling is almost independent of it because $\rho \sim \gamma/N$ for small K in the second term of Eq. (33).
- (iii) When the (positive) coupling is introduced, ρ for the sigmoid coupling is increased while ρ for the diffusive coupling is independent of it.
- (iv) With increasing the (positive) coupling strength, the ratio of ρ/γ is increased for both the couplings. This leads to an increased synchronization ratio of S(t):

$$S(t) = \left(\frac{\rho(t)/\gamma(t) - 1/N}{1 - 1/N}\right) = \left(\frac{N\rho(t) - \gamma(t)}{(N - 1)\gamma(t)}\right),\tag{41}$$

which is one and zero for the completely synchronous and asynchronous states, respectively [4][25].

2.5 Nature of the AMM

Before proceeding to the next section of numerical results, we will discuss the nature of the AMM, which is essentially the second-moment approximation for local and global variables. One of disadvantages of the AMM is that its applicability is limited to the weak-noise case because higher-order moments are assumed to be neglected. The second-moment given by Eq. (10) is positive definite for the magnitude of the multiplicative noise α , as given by

$$\langle x^2 \rangle = \frac{\beta^2}{2(\lambda - \alpha^2)} < +\infty, \quad \text{for } \alpha^2 < \lambda$$
 (42)

in the case of I = J = K = 0. A simple calculation leads to the equation of motion of the k-th moment for even k given by

$$\frac{\partial \langle x^k \rangle}{\partial t} = -\left(k\lambda - \frac{k^2\alpha^2}{2}\right)\langle x^k \rangle + \frac{k(k-1)\beta^2}{2}\langle x^{k-2} \rangle, \qquad (k=2,4,\cdots)$$
 (43)

from which the stationary value of $\langle x^k \rangle$ is given by

$$\langle x^k \rangle = \frac{(k-1)\beta^2}{2(\lambda - k\alpha^2/2)} \langle x^{k-2} \rangle,$$
 (44)

$$= \frac{(k-1)!! \,\beta^k}{2^{k/2} \prod_{\ell=1}^{k/2} (\lambda - \ell \,\alpha^2)}.$$
 (45)

We get the positive definite $\langle x^k \rangle$ for $\alpha^2 < 2\lambda/k$, which implies that for $2\lambda/k < \alpha^2 < \lambda$ with $k \geq 4$, the k-th moment may diverge even if $\langle x^2 \rangle$ remains finite. This might throw some doubt on the validity of the AMM for the multiplicative noise. Equations (43) expresses that the motion of $\langle x^k \rangle$ depends on those of its lower moments ($\leq k-2$), but does not on its higher moments ($\geq k+2$). Even if $\langle x^4 \rangle$ diverges, for example, it has no effects on the motion of $\langle x^2 \rangle$. We hope that our AMM is meaningful and useful for discussions on stochastic systems subjected to multiplicative noise, because the results of the AMM are in good agreement with those of DS, as will be demonstrated in our numerical calculations. The advantage of the AMM is that we can easily discuss the dynamics of N-unit Langevin model by solving the three-dimensional ordinary differential equations. Note that it is much more tedious to solve (N+1)-dimensional partial differential equations in FPE and N-dimensional stochastic equations in DS.

3 Numerical results

3.1 Stationary property

3.1.1 Size (N) dependence

We have performed numerical calculations for linear Langevin models, solving AMM equations by the Runge-Kutta method with a time step of 0.01. Direct simulations for the N-unit Langevin model have been performed by using the Heun method with a time step of 0.0001. Results shown in the paper are averages of 1000 trials otherwise noticed.

The N-dependences of γ and ρ in the stationary states for the diffusive couplings of $J=0.0,\ 0.2$ and 0.5 are plotted in Fig. 1(a) where solid curves and marks denote the results of the AMM and DS, respectively. We note that for $J=0,\ \rho$ is inversely proportional to N, as realized in Eq. (29). With increasing $J,\ \gamma$ is decreased while ρ has no changes. The results of AMM are in good agreement with those of DS.

The N-dependences of γ and ρ in the stationary states for sigmoid couplings of K = 0.0, 0.2 and 0.5 are plotted in Fig. 1(b) where solid curves denote the result of the AMM [Eqs.(36) and (38)] and where marks express those of DS calculated by using H(x) = x. With increasing K, ρ is increased while γ is little changed except for N < 5.

3.1.2 Noise-strength (α) dependence

The α dependences of stationary γ and ρ for diffusive couplings with N=10, $\lambda=1.0$ and $\beta=1.0$ are shown in Figs. 2(a), where filled and open marks denote γ and ρ , respectively, in DS, and solid and chain curves the respective results in the AMM. Note that the results of ρ are multiplied by a factor of 10~(=N), and that three curves in the AMM are degenerated in Fig. 2(a): $10\rho(J=0.5)=10\rho(J=0.0)=\gamma(J=0.0)$. For J=0.0, the relation of $\rho=\gamma/N$ holds in both the AMM and DS. For J=0.5, γ in the AMM is decreased compared to that for J=0.0, in agreement with the result of DS. In contrast, ρ in the AMM is the same as that of J=0.0 because it is independent of J [Eq. (25)], while ρ in DS is decreased with increasing J at $\alpha>0.6$. The results of the AMM diverge at $\alpha=1$, where those of DS remain finite. This difference in ρ between the AMM and DS at large α is attributed to the second-moment approximation in the AMM, and it is the fallacy in the AMM neglecting higher-order moments.

Figure 2(b) shows the α -dependent γ and ρ for the sigmoid couplings of K=0.5. Solid and chain curves denote γ and ρ , respectively, in the AMM given by Eqs. (36) and (38): filled and open squares express those in DS with H(x)=x. Although γ and ρ diverge at $\alpha = 0.71$ in the AMM, they persist up to $\alpha \sim 0.77$ in DS.

3.1.3 Coupling (J, K) dependence

Figure 3(a) shows the J dependences of γ and ρ for the diffusive couplings with N=10, $\alpha=0.5$ and $\beta=1.0$: solid and chain curves express γ and ρ , respectively, in the AMM, and filled and open circle the respective results in DS. With increasing J, γ is decreased while ρ is almost independent of J.

The K dependences of γ and ρ for the sigmoid couplings are plotted in Fig. 3(b) where solid and chain curves express γ and ρ , respectively, in the AMM, and filled and open circle denote γ and ρ , respectively, in DS. In the AMM, the critical coupling K_c where γ and ρ diverge, is $K_c = 0.75$ [Eqs.(36) and (38)] while DS leads to $K_c \sim 0.84$.

These differences realized in numerical results are consistent with the items (ii) and (iii) mentioned in Section 2.3. We note in Figs. 3(a) and 3(b) that the synchronization is increased with increasing J and K because Eq. (41) approximately yields $S \propto (10\rho - \gamma)$: S is proportional to the difference between chain (10ρ) and solid curves (γ) . This agrees with the item (iv) in Section 2.3 denoting the similarity between the two couplings.

3.2 Dynamical property

We apply a pulse input given by

$$I^{(e)}(t) = A \Theta(t - t_1)\Theta(t_2 - t), \tag{46}$$

with A=0.5, $t_1=40$ and $t_2=50$, where $\Theta(x)$ denotes the Heaviside function: $\Theta(x)=1$ for x>0 and zero otherwise. Figures 4(a), 4(b) and 4(c) show the responses of $\mu(t)$, $\gamma(t)$ and $\rho(t)$, respectively, to the external input given by Eq. (46) with $\alpha=0.5$, $\beta=1.0$, J=0.0 and N=10. Solid curves denote the results of the AMM which are in good agreement with those of DS. Input pulse induces changes not only in $\mu(t)$ but also in $\gamma(t)$ and $\rho(t)$. These arise from terms of $\alpha^2 \mu^2$ in Eqs. (24) and (25). Indeed, in the case of $\alpha=0.0$, input pulse induces no changes in $\gamma(t)$ and $\rho(t)$, as shown by chain curves for the AMM result.

The response of $\mu(t)$ for the diffusive coupling is independent of the coupling J, as realized in Eq. (23). In contrast, the response $\mu(t)$ for the sigmoid coupling shows much variety depending on its coupling K. Figure 5(a) and 5(b) show $\mu(t)$ and S(t), respectively, for various values of K with $\alpha = 0.5$, $\beta = 0.0$ and N = 10, when the pulse input given by Eq. (46) is applied. With increasing K, magnitudes of $\mu(t)$ are increased at 40 < t < 50

during which the input pulse is applied. It is interesting that the synchronization S(t) is decreased at 40 < t < 50 by an applied input pulse which reduces the ratio of ρ/γ , and then S(t) is much increased at t > 50. For K = 0.0, S(t) vanishes because $\rho = \gamma/N$ in Eq. (41). Figure 5(c) and 5(d) show similar plots of $\mu(t)$ and S(t), respectively, for combined noises of $\alpha = 0.5$ and $\beta = 1.0$. With increasing K, the magnitude of $\mu(t)$ is again increased, although an agreement between the results of the AMM and DSs become worse than that shown in Fig. 5(a). S(t) is decreased by an applied pulse, but no increases at t > 50, in contrast with the case shown in Fig. 5(b).

We have applied also the sinusoidal input given by

$$I^{(e)}(t) = A \left[1 - \cos\left(\frac{2\pi t}{T_p}\right) \right],\tag{47}$$

where A=0.5 and $T_p=20$. The responses of $\mu(t)$, $\gamma(t)$ and $\rho(t)$ are shown in Figs. 6(a), 6(b) and 6(c), respectively, when the external input given by Eq. (46) is applied for $\alpha=0.5$, $\beta=1.0$, J=0.0 and N=10. Solid curves expressing the results of the AMM are in good agreement with dashed curves of those of DS. Input pulse induces changes in $\mu(t)$ and also in $\gamma(t)$ and $\rho(t)$. For a comparison, we show, by chain curves, the AMM result for $\alpha=0.0$, for which no changes in $\gamma(t)$ and $\rho(t)$ by an applied input.

4 DISCUSSION AND CONCLUSION

It is interesting to discuss the stationary distribution of our generalized Langevin model given by Eqs. (1)-(3). In the case of no couplings (J = K = 0), the probability distribution $\hat{p}(\{x_i\}, t)$ is given by

$$\hat{p}(\{x_i\}, t) = \prod_i p(x_i, t), \tag{48}$$

where $p(x_i, t)$ expresses the distribution for a local variable x_i satisfying the FPE given by

$$\frac{\partial}{\partial t} p(x_i, t) = -\frac{\partial}{\partial x_i} \{ [F(x_i) + \frac{\phi \alpha^2}{2} G'(x_i) G(x_i) + I^{(e)}] p(x_i, t) \}
+ \frac{1}{2} \frac{\partial^2}{\partial x_i^2} \{ [\alpha^2 G(x_i)^2 + \beta^2] p(x_i, t) \}.$$
(49)

For a constant input of $I^{(e)}(t) = I$, the stationary distribution $p(x_i)$ is expressed by [12]-[15]

$$\ln p(x) = X(x) + Y(x) - \left(1 - \frac{\phi}{2}\right) \ln \left[\frac{\alpha^2 G(x)^2}{2} + \frac{\beta^2}{2}\right], \tag{50}$$

with

$$X(x) = 2 \int dx \left[\frac{F(x)}{\alpha^2 G(x)^2 + \beta^2} \right], \tag{51}$$

$$Y(x) = 2 \int dr \left[\frac{I}{\alpha^2 G(x)^2 + \beta^2} \right]. \tag{52}$$

For the linear Langevin model with $F(x) = -\lambda x$ and G(x) = x, p(x) in the Stratonivich representation becomes

$$p(x) \propto \left[1 + \left(\frac{\alpha^2}{\beta^2}\right) x^2\right]^{-(\lambda/\alpha^2 + 1/2)} \exp[Y(x)],$$
 (53)

with

$$Y(x) = \left(\frac{2I}{\alpha\beta}\right) \arctan\left(\frac{\alpha x}{\beta}\right). \tag{54}$$

We examine the some limiting cases of Eq. (53) as follows.

(a) Equation (53) in the case of I = Y(x) = 0 expresses the q-Gaussian [13, 14, 26, 27], which becomes, in the limit of large $x \gg \beta/\alpha$,

$$p(x) \propto x^{-\delta},$$
 (55)

with

$$\delta = \frac{2\lambda}{\alpha^2} + 1. \tag{56}$$

The expectation value of x^2 is given by

$$\langle x^2 \rangle = \frac{\beta^2}{2(\lambda - \alpha^2)},\tag{57}$$

which requires $\alpha^2 < \lambda$ for positive definite $\langle x^2 \rangle$.

(b) For $\alpha = 0$ and $\beta \neq 0$, we get from Eq. (53)

$$p(x) \propto \exp\left[-\left(\frac{\lambda}{\beta^2}\right)\left(x - \frac{I}{\lambda}\right)^2\right].$$
 (58)

(c) For $\beta = 0$ and $\alpha \neq 0$, Eq. (53) becomes

$$p(x) \propto x^{-(2\lambda/\alpha^2+1)} \exp\left[-\left(\frac{2I}{\alpha^2}\right)\frac{1}{x}\right].$$
 (59)

Figures 7(a)-7(c) show the distribution p(x) calculated with the use of Eqs. (53)-(59). The distribution p(x) for $\alpha = 0.0$ in Fig. 7(a) shows the Gaussian distribution given by Eq. (58) without multiplicative noises, which is shifted by an applied input I. When

multiplicative noises are added ($\alpha \neq 0$), the form of p(x) is changed but the average of $\langle x \rangle$ is conserved as shown in Fig. 7(a). Figure 7(b) shows that when the magnitude of additive noises β is increased, the width of p(x) is increased. We note in Fig. 7(c) that although p(x) is symmetric for I = 0, the external input I increases the asymmetry in p(x). Figures 7(a)-7(c) clearly show that p(x) is much modified by the presence of I.

Now we consider the averaged, global variable X(t) given by Eq. (8). The stationary distribution for a global variable X given by Eq. (9), is analytically expressed only for limited cases.

(a) For $\beta \neq 0$ and $\alpha = 0$, P(X) is given by

$$P(X) \propto \exp\left[-\left(\frac{\lambda N}{\beta^2}\right)\left(X - \frac{I}{\lambda}\right)^2\right],$$
 (60)

which arises from the central-limit theorem for β .

(b) For I = 0, we get

$$P(X) = \frac{1}{2\pi} \int_{-\infty}^{\infty} dk \ e^{ikX} \Phi(k), \tag{61}$$

with

$$\Phi(k) = \left[\phi\left(\frac{k}{N}\right)\right]^N,\tag{62}$$

where $\phi(k)$ is the characteristic function for p(x) given by [28]

$$\phi(k) = \int_{-\infty}^{\infty} e^{-ikx} p(x) dx, \qquad (63)$$

$$= 2^{1-\nu} \frac{(\lambda' \mid k \mid)^{\nu}}{\Gamma(\nu)} K_{\nu}(\lambda' \mid k \mid), \tag{64}$$

with

$$\nu = \frac{\lambda}{\alpha^2},\tag{65}$$

$$\lambda' = \frac{\beta}{\alpha},\tag{66}$$

 $K_{\nu}(x)$ expressing the modified Bessel function.

The asymptotic form of P(X) for large X and large N is obtained as follows. By using the relation:

$$z^{\nu}B_{\nu}(z) \propto \left[1 - cz^2 - dz^{2\nu} + \cdots\right], \quad \text{for } z \ll 1, \ \nu \neq 1$$
 (67)

with

$$c = \frac{1}{4(\nu - 1)},\tag{68}$$

$$d = \left(\frac{1}{2}\right)^{2\nu} \frac{\Gamma(1-\nu)}{\Gamma(1+\nu)},\tag{69}$$

we get, for large N,

$$\Phi(k) \propto \exp(-a_N k^2), \qquad \text{for } \nu > 1$$
(70)

$$\propto \exp(-b_N \mid k \mid^{2\nu}), \quad \text{for } 0 < \nu < 1$$
 (71)

with

$$a_N = cN^{-1}(\lambda')^2, (72)$$

$$b_N = dN^{1-2\nu} (\lambda')^{2\nu}. \tag{73}$$

For large X, Eqs. (61), (70)-(73) yield

$$P(X) \propto \exp\left(-\frac{X^2}{2\sigma_N^2}\right), \quad \text{for } \nu > 1$$
 (74)

$$\propto X^{-\delta'}, \qquad \text{for } 0 < \nu < 1$$
 (75)

with

$$\sigma_N^2 = 2a_N = \frac{\beta^2}{2N(\lambda - \alpha^2)},\tag{76}$$

$$\delta' = 2\nu + 1 = \frac{2\lambda}{\alpha^2} + 1. \tag{77}$$

It is interesting that for N=1, Eq. (76) coincides with Eq. (57) and the index of δ' given by Eq. (77) is the same as δ given by Eq. (56). The case of $\nu=1$, excluded in the above analysis, will be numerically studied below. The stable distribution of P(X') for $X'(t) = N^{-1/2\nu} \sum_i x_i(t)$ with $0 < \nu < 1$ was discussed in Ref. [28].

Figures 8(a) shows distributions of a global variable P(X) for I=0.0 calculated by DS for the Langevin model given by Eq. (1) with N=1, N=10 and N=100 ($\lambda=1.0$, $\alpha=1.0$, $\beta=0.5$ and $\nu=1.0$). For a comparison, results of the analytic expression given by Eqs. (61), (62) and (64) are plotted with a shift by X=-2 for a clarity of the figure. We note that with increasing N, the width of P(X) becomes narrower, which is consistent with the central-limit theorem. Figures 8(b) and 8(c) show P(X) for I=1.0 and I=2.0, respectively, calculated by DS. The N dependence of P(X) for finite I is intrigue: with increasing N, not only its width becomes narrower but also its profile is considerably modified, as shown in Figs. 8(b) and 8(c). This trend is more significant for a larger I.

So far we have assumed the vanishing couplings, which is now introduced. Figure 9(a) shows distributions of p(x) and P(X) for the diffusive couplings of J = 0.0 (dashed

curves) and J = 1.0 (solid curves) with I = 0.0. We note that with increasing J, the width of p(x) becomes narrower while that of P(X) is not changed. This is the case also for finite I = 1.0, as shown in Fig. 9(b).

Figure 9(c) shows p(x) and P(X) with I=0 for the sigmoid coupling of K=0.0 (dashed curve) and K=0.5 (solid curve). We note that the width of P(X) for K=0.5 become wider than that for K=0.0. Figure 9(d) shows that an introduction of K with finite I=1.0 induces not only an increase in the width of P(X) but also its shift. This is in contrast with the case of the diffusive coupling shown in Fig. 9(b), where P(X) has little effects of J.

The coupling dependences of stationary distributions of p(x) and P(X) are related to those of γ and ρ , because $\sqrt{\gamma}$ and $\sqrt{\rho}$ approximately express the widths of p(x) and P(X), respectively. Figure 9(a) shows that with increasing J, the width of p(x) is decreased while that of P(X) is unchanged for the diffusive couplings. In contrast, for the sigmoid coupling, the width of P(X) is increased while that of p(x) is unchanged when K is increased, as shown in Fig. 9(c). These are consistent with the dependences of γ and ρ on the type of couplings expressed in the items (ii) and (iii) having been discussed in Section 2.3.

5 CONCLUSION

By using the AMM, we have studied stationary and dynamical properties of finite N-unit Langevin model which is subjected to multiplicative noises and which is coupled by diffusive and sigmoid couplings. Properties of coupled Langevin model are shown to depend on both the type and magnitude of couplings, which is the same as in the case of FitzHugh-Nagumo model [9][29]. One of advantages of the AMM is that we may easily solve the low-dimensional differential equations although its applicability is limited to the weak-noise case. It would be interesting to apply the AMM to various types of stochastic coupled ensembles such as neuronal and complex networks in order to discuss their dynamics.

Acknowledgements

This work is partly supported by a Grant-in-Aid for Scientific Research from the Japanese Ministry of Education, Culture, Sports, Science and Technology.

References

- [1] B. Lindner, J. García-Ojalvo, A. Neiman, and L. Schimansky-Gelier, Physics Report **392** (2004) 321.
- [2] H. Risken: The Fokker-Planck Equation: Methods of Solution and Applications, Springer Series in Synergetics, Vol. 18 (Springer Verlag, Berlin, 1992).
- [3] R. Rodriguez and H. C. Tuckwell, Phys. Rev. E **54** (1996) 5585.
- [4] H. Hasegawa: Phys. Rev E **67** (2003) 041903.
- [5] H. Hasegawa, Phys. Rev E 68 (2003) 041909.
- [6] H. Hasegawa, Phys. Rev. E 70 (2004) 021911.
- [7] H. Hasegawa, Phys. Rev. E 70 (2004) 021912.
- [8] H. Hasegawa, Phys. Rev. E 70 (2004) 066107.
- [9] H. Hasegawa, Phys. Rev. E 72 (2005) 056139.
- [10] H. Hasegawa, J. Phys. Soc. Jpn. **75** (2006) 033001; the third term of Eq. (17) in this reference should be $(w/Z) \sum_k [\langle x_i x_k \rangle + \langle x_j x_k \rangle 2 \langle x_i x_j \rangle]$.
- [11] M. A. Muñoz: in 'Advances in Condensed Matter and Statistical Mechanics', edit by E. Korutcheva and R. Cuerno (Nova Science Publishers, New York, 2004), p. 34.
- [12] A. Schenzle and H. Brandt, Phys. Rev. A **20** (1979) 1628.
- [13] H. Sakaguchi: J. Phys. Soc. Jpn. **70** (2001) 3247.
- [14] C. Anteneodo and C. Tsallis: J. Math. Phys. 44 (2003) 5194.
- [15] C. Anteneodo and R. Riera, Phys. Rev. E 72 (2005) 026106.
- [16] C. Van den Broeck, J. M. R. Parrondo, and R. Toral, Phys. Rev. Lett. 73 (1994) 3395.
- [17] C. Van den Broeck, J. M. R. Parrondo, R. Toral, and R. Kawai: Phys. Rev. E 55 (1997) 4084.

- [18] T. Birner, K. Lippert, R. Müller, A. Kühnel, and U. Behn, Phys. Rev E 65 (2002) 046110.
- [19] R. Kawai, X. Sailer, L. Schimansky-Geier, and C. Van den Broeck: Phys. Rev E 69 (2004) 051104.
- [20] M. A. Muñoz, F. Colaiori, and C. Castellano: Phys. Rev. E 72 (2005) 056102.
- [21] G. Wilk and Z. Wlodarczyk, Phys. Rev. Lett. 84 (2000) 2770.
- [22] H. Hasegawa: Physica A **365** (2006) 383.
- [23] L. H. A. Monteiro, M. A. Bussab, J. G. C. Berlinck, J. Theor. Biol. 219 (2002) 83.
- [24] H. Haken: Advanced Synergetics (Springer-Verlag, Berlin, 1983); the multiplicative-noise term in FPE given by Eq. (7) is derived from eqs. (4.2.24) and (4.3.18) in this reference with $g_{km} = \alpha G(x_k) \delta_{km}$.
- [25] First we consider the quantity given by $P(t) = N^{-2} \sum_{ij} \langle [x_i(t) x_j(t)]^2 \rangle = 2[\gamma(t) \rho(t)]$, which is zero for the completely synchronous state and which is $2(1 1/N)\gamma$ ($\equiv P_0$) for the completely asynchronous states. The synchronization ratio given by Eq. (41) is defined by S(t) (= $1 P(t)/P_0(t)$), which is zero (one) for completely asynchronous (synchronous) state [4].
- [26] C. Tsallis: J. Stat. Phys. **52** (1988) 479.
- [27] C. Tsallis, R. S. Mendes, and A. R. Plastino: Physica A 261 (1998) 534.
- [28] S. Abe and A. K. Rajagopal: J. Phys. A: Math. Gen. **33** (2000) 8723.
- [29] H. Hasegawa: cond-mat/0601358.

- Figure 1: (Color online) (a) The N dependences of the stationary γ and ρ for various diffusive couplings (DC): circles, triangles and square denote results of DS for J=0.0, J=0.2 and J=0.5, respectively, and solid curves express those of the AMM. (b) The N dependence of the stationary γ and ρ for various sigmoid couplings (SC) with H(x)=x: circles, triangles and square denote results of DS for K=0.0, K=0.2 and K=0.5, respectively, solid curves express those of the AMM ($\lambda=1.0$, $\alpha=0.5$ and $\beta=1.0$). Dashed curves are drawn only for a guide of the eye.
- Figure 2: (Color online) (a) The α dependences of the stationary γ (solid curves) and ρ (chain curves) for the diffusive couplings (DC): circles, triangles and square denote results of DS for J=0.0 and J=0.5, respectively, and solid and chain curves express those of the AMM. (b) The α dependence of the stationary γ (solid curves) and ρ (chain curves) for sigmoid couplings (SC) of K=0.5 with H(x)=x: squares denote results of DS, and solid and chain curves express those of the AMM. (N=10, N=1.0 and N=1.0). Dashed curves are drawn only for a guide of the eye.
- Figure 3: (Color online) (a) The J dependences of the stationary γ (solid curves) and ρ (chain curves) for the diffusive couplings (DC): circles denote results of DS, and solid and chain curves express those of the AMM. (b) The K dependence of the stationary γ (solid curves) and ρ (chain curves) for sigmoid couplings (SC) with H(x) = x: squares denote results of DS, and solid and chain curves express those of the AMM. (N = 10, $\lambda = 1.0$, $\alpha = 0.5$ and $\beta = 1.0$). Dashed curves are drawn only for a guide of the eye.
- Figure 4: (Color online) Responses of (a) $\mu(t)$, (b) $\gamma(t)$ and (c) $\rho(t)$ to the pulse input with $J=0.0,\ N=10,\ \lambda=1.0,$ and $\beta=1.0$: solid and dashed curve denote results of AMM and DS, respectively, for $\alpha=0.5,$ and chain curves express that of AMM for $\alpha=0.0.$
- Figure 5: (Color online) (a) Responses of $\mu(t)$ and (b) S(t) to the pulse input for various sigmoid couplings with $\lambda = 1.0$, $\alpha = 0.5$, $\beta = 0.0$ and N = 10. (c) Responses of $\mu(t)$ and (d) S(t) to the pulse input for various sigmoid couplings with $\lambda = 1.0$, $\alpha = 0.5$, $\beta = 1.0$ and N = 10. Solid and dashed curves denote results of AMM and DS, respectively.
- Figure 6: (Color online) Responses of (a) $\mu(t)$, (b) $\gamma(t)$ and (c) $\rho(t)$ to the sinusoidal input with J=0.0, N=10, $\lambda=1.0$, and $\beta=1.0$: solid and dashed curve denote results of AMM and DS, respectively, for $\alpha=0.5$, and chain curves express that of AMM for $\alpha=0.0$.
- Figure 7: (a) Distributions p(x) of local variable x for various α with $\lambda = 1.0$, $\beta = 1.0$ and I = 1.0, (b) p(x) for various β with $\lambda = 1.0$, $\alpha = 1.0$ and I = 1.0, and (c) p(x) for various I with $\lambda = 1.0$, $\alpha = 1.0$ and $\beta = 0.5$.

Figure 8: (Color online) Distributions P(X) of global variable X calculated by direct simulation (DS) for N=1 (dashed curves), N=10 (solid curves) and N=100 (chain curves) with (a) I=0, (b) I=1.0 and (c) I=2.0 ($\lambda=1.0$, $\alpha=1.0$ and $\beta=0.5$). Results calculated with the use of Eqs. (67), (68) and (70) are plotted in (a) with a shift of X=-2 for a clarity of the figure.

Figure 9: (Color online) Distributions of p(x) and P(X) of local and global variables, respectively, with (a) I=0.0 and (b) I=1.0 for diffusive coupling (DC) with J=0.0 (dashed curves) and J=1.0 (solid curves), and those with (c) I=0.0 and I=1.0 for sigmoid coupling (SC) with K=0.0 (dashed curves) and K=0.5 (solid curves). (N=10, $\lambda=1.0$, $\alpha=0.5$ and $\beta=1.0$).

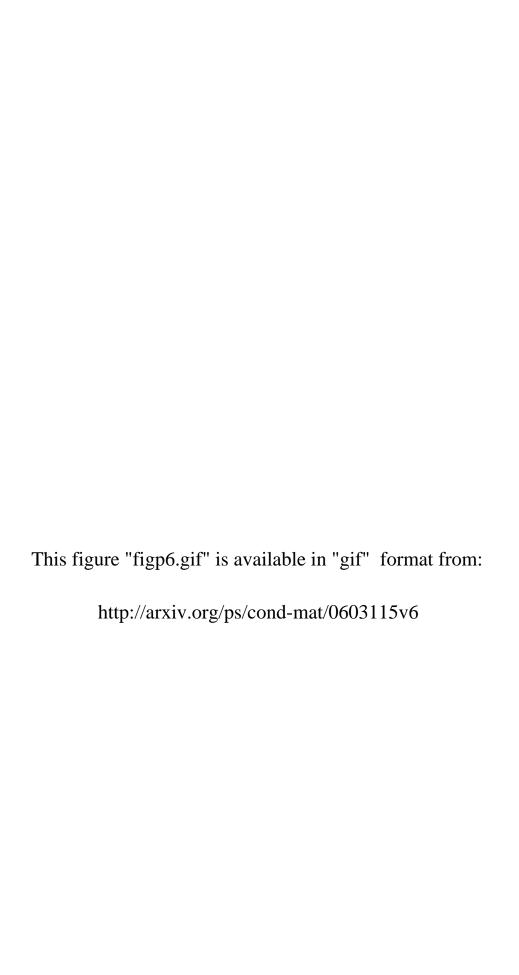
This figure "figp1.gif" is available in "gif" format from:

This figure "figp2.gif" is available in "gif" format from:

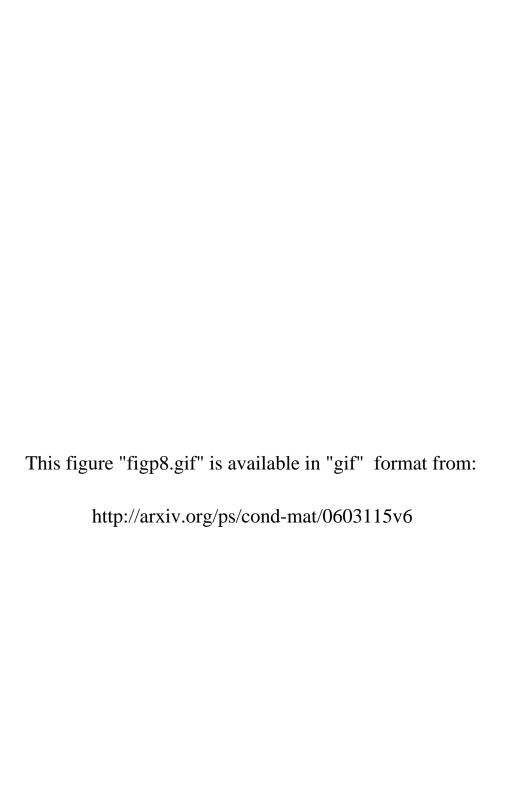
This figure "figp3.gif" is available in "gif" format from:

This figure "figp4.gif" is available in "gif" format from:

This figure "figp5.gif" is available in "gif" format from:



This figure "figp7.gif" is available in "gif" format from:



This figure "figp9.gif" is available in "gif" format from: